GFRP hollow column to built-up beam adhesive connection: mechanical behaviour under quasi-static, cyclic and fatigue loading

Razaqpur AG[(1)], Ascione F[(2)], Lamberti M[(3,*)], Spadea S[(4)], Malagic M[(5)]

(1) College of Environmental Science and Engineering, Nankai University, Tianjin, China, email: *GRazaqpur@nankai.edu.cn*
(2) Dept. of Civil Engineering, University of Salerno, Italy, email: *fascione@unisa.it*
(3) College of Environmental Science and Engineering, Nankai University, Tianjin, China, email: *mlamberti@nankai.edu.cn*
(4) School of Science and Engineering, University of Dundee, United Kingdom, email: *s.spadea@dundee.ac.uk*
(5) Fiberline Composites A/S. Barmstedt Allé 5. DK-5500 Middelfart, email: *mma@fiberline.com*

**Corresponding author*

Abstract

A new adhesive beam-column connection is tested which possess the highest strength and stiffness compared to any other similar adhesive or bolted connection tested in the past. A square GFRP hollow section, acting as a column, was connected to a built-up beam made of two GFRP U-profiles by means of either epoxy or steel bolts. The beam-column assembly formed an L-shaped frame which was tested by applying a point load at the beam free end while the column was fixed at its base. Five bolted and five adhesive replicate connections were subjected to quasi-static loading up to failure. Another three adhesive connections were subjected to 400, 800 or 1200 cycles of loading and unloading with the maximum load being equal to 0.50 $P_{u,avg}$, where $P_{u,avg}$ is the average static strength of the replicate adhesive specimens. At the end of the cyclic loading, the latter specimens were loaded quasi-statically to failure. Finally, another two adhesive connections were subjected to fatigue type loading. They were successively subjected to at least 196 cycles of loading and unloading with the load amplitude being 0.50 $P_{u,avg}$ in the first 60 cycles, 0.75 $P_{u,avg}$ in the next 60 cycles, 0.85 $P_{u,avg}$ in the following 60 cycles and 0.95 $P_{u,avg}$ after the 180^{th} cycle. The test results show that the proposed adhesive connection can achieve on average 82% higher strength and 380% higher rotational stiffness than the companion bolted connection. Furthermore, the above cyclic loading has negligible effect on either the strength or the stiffness of the connection. Finally, the connection can sustain the foregoing fatigue load up to almost 180 cycles without significant damage but it will not be able to withstand the full 60 cycles of the load with 0.95 $P_{u,avg}$ amplitude. The current results demonstrate the superior strength and stiffness of the new adhesive connection compared to a similar bolted connection.

Keywords: GFRP, Adhesive and Bolted joints, Cyclic, Fatigue, Stiffness, Strength.

1. Introduction

Fibre reinforced polymer (FRP) materials are appealing as alternative to traditional construction materials due to their high tensile strength, excellent resistance to aggressive environments [1–5], high strength to weight ratio, simple and rapid installation time. Also, due to their low maintenance requirements, these materials offer a promising alternative for the development of more durable and sustainable structures [6-7]. Moreover, through suitable combinations of matrix and fibers it is possible to tailor make composite materials to optimally meet specific design requirements.

Presently, pultrusion is the preferred method for production of continuous FRP profiles with constant cross-section, such as hollow sections, angles, I-beams and channels, all being suitable for construction of frame type structures. FRP composites can be made with carbon, glass, basalt or aramid fibers, but glass fibre is commonly used for fabrication of composites materials used in the construction industry due to its relatively lower cost compared to the other types of fibre [8].

"This is a post-peer-review, pre-copyedit version of an article published in [Composite Structures]. The final authenticated version is available online at https://doi.org/10.1016/j.compstruct.2019.111069

Although glass FRP (GFRP) members have high strength and reasonable stiffness, a functional and safe frame structures also require reliable connection systems between the structural members, including beam-to-column connection.

Efforts to develop suitable connection systems for GFRP members started at least three decades ago [9-15] and continue to this day [16-18]. In many previous investigations, GFRP I-sections have been used as beams and columns, mimicking the practice in steel structures construction. Also, most of the investigations have focused on bolted connections between GFRP I-beams and columns. Connection configurations that have been studied include GFRP and/or steel shelf angles, bolted to GFRP beams and columns either by bolts only or by bolts and epoxy resin. An extensive overview of the current state of art is presented by Ascione et al. [19]. The results show that such connections experience brittle failure initiated by the detachment of the column flange from the web and delamination in the corner of top shelf angles.

Recently, the present authors have conducted experimental investigations [19] to demonstrate the structural effectiveness of adhesively bonded connections between pultruded I-profiles. The test results show that bonded connections, if properly designed and constructed, can achieve high strength capacity, at least comparable to the best available bolted connection [19]. Consequently, the limitations imposed by current design guidelines on the use of adhesive beam-column connections in GFRP frame structures appear unwarranted [20]. However, a key disadvantage of the adhesive connection is the brittle failure of the adhesive joining the members, which limits the deformability of framed GFRP structures. To overcome this drawback, the authors have proposed a modified connection [21] which features wrapping some parts of the connection by carbon FRP laminate. Such strengthened connection exhibited a pseudo-ductile load-deflection response.

Based on first principles and as demonstrated by Smith et al. [12], GFRP sections with closed shapes (i.e., tubular sections) provide certain mechanical properties that are superior to open shapes (I-shaped sections), such as higher local flange buckling load, higher torsional rigidity, and higher weak axis strength and stiffness. GFRP frames made of box sections have been found to have 25% higher connection stiffness and 280% higher strength vis-à-vis I-shaped sections with the same bending stiffness. Accordingly, the optimal connection between tubular profiles has become the focus of research by several investigators [22-26]. For example, a bonded sleeve connection system was recently proposed for GFRP beam-column. The experimental investigation by Wu et al [22] and the numerical study by Zhang et al. [23] show the improved moment capacity and rotational stiffness of tubular FRP-steel bonded sleeve connection over steel seated angle connections and bolted sleeve connections. The performance of such connection was also explored by Zhang et al. under static [24] and cyclic loading [25] for FRP beam-to-column assemblies. Martins et al. [26] developed an innovative beam-to-column bolted connection system for GFRP tubes, comprising purpose-built steel connection elements to be inserted into the GFRP hollow sections. Four different bolt configurations were tested, including the number and distance of the bolts from the connected beam end. The investigation took into account: (i) one bolt per web, (ii) two bolts per flange and short end distance, (iii) four bolts per flange, (iv) two bolts per flange and a longer end distance. The study demonstrates that maximum rotational stiffness is provided by the configuration (iii) and the maximum failure load by configuration (iv).

The foregoing investigations have focused on bolted connections using steel bolts alone or steel bolts in conjunctions with epoxy adhesive. But there are reasons to believe that adhesive connections by themselves can achieve higher strength and better performance compared to bolted connections in FRP composite structures. Firstly, it is well known that the holes made in structural members cause stress concentration and increase the risk of moisture penetration within the matrix-fibre interface. Also, as discussed in [19], current moment resisting bolted beam-column connections in GFRP structures can rarely resist more than 20% of the flexural capacity of the connected members, with failure initiated by high local bearing stresses. On the other hand, it has been observed that stresses are relatively uniformly distributed over the bonded surfaces in simple

"This is a post-peer-review, pre-copyedit version of an article published in [Composite Structures]. The final authenticated version is available online at https://doi.org/10.1016/j.compstruct.2019.111069

bonded lap joint connections due to the absence of stress concentration and fibre discontinuity caused by the introduction of holes. While bonded lap joints have been extensively investigated in composites, for beam-to-column bonded connections there are few experimental or numerical results available to assess their strength, stiffness and overall performance. To fill this gap in knowledge, the objective of this paper is to experimentally characterize the behaviour of an adhesive GFRP connection between a tubular profile (column) and a built-up beam composed of U-profiles. As stated earlier, the choice of tubular profile for the the column is motivated by the increased torsional stiffness and resistance to distortion as well as the greater available surface for bonding.
To investigate the strength, stiffness and fatigue strength of the connection, it will be tested under static and cyclic loads. The connection response under static load will be compared to the behaviour of an analogous bolted connection to demonstrate the better overall performance of the former.

2. Experimental Program

The investigated connections join a tubular column made of a commercially available hollow GFRP profile with square cross section (120 x 120 x 6 mm) and two U-profiles (160 x 48 x 8 x 5 mm) arranged together in the form of a built-up beam. Both the beam and the column are 500 mm long.
For comparison, the members were joined using both adhesive and bolted connections as described below. The material properties used in the current investigation are based on the test results, as reported in [19,21], performed by the authors at the Laboratory of Materials and Structural Testing of the University of Salerno (Italy).
The former results were found to be in close agreement with the manufacturer's published data [27].

2.1 Design and preparation of adhesive joints

Ten full scale test specimens were constructed as illustrated in Figure 1. An epoxy-based adhesive, called SikaDur 30 [28], was used for bonding the connected elements. The adhesive thickness was typically 1 to 2 mm. To maximise the bonded surface area, four 50 x 50 x 6 mm angle profiles were positioned at the bottom and the top of the two U-profiles as indicated in Figure 1(b). Furthermore, to minimize possible lateral bucking, the two profiles were also connected to each other at their free ends by means of a 100 mm long 120 x 120 x 6 mm square tube inserted between the two profiles and bonded to them.

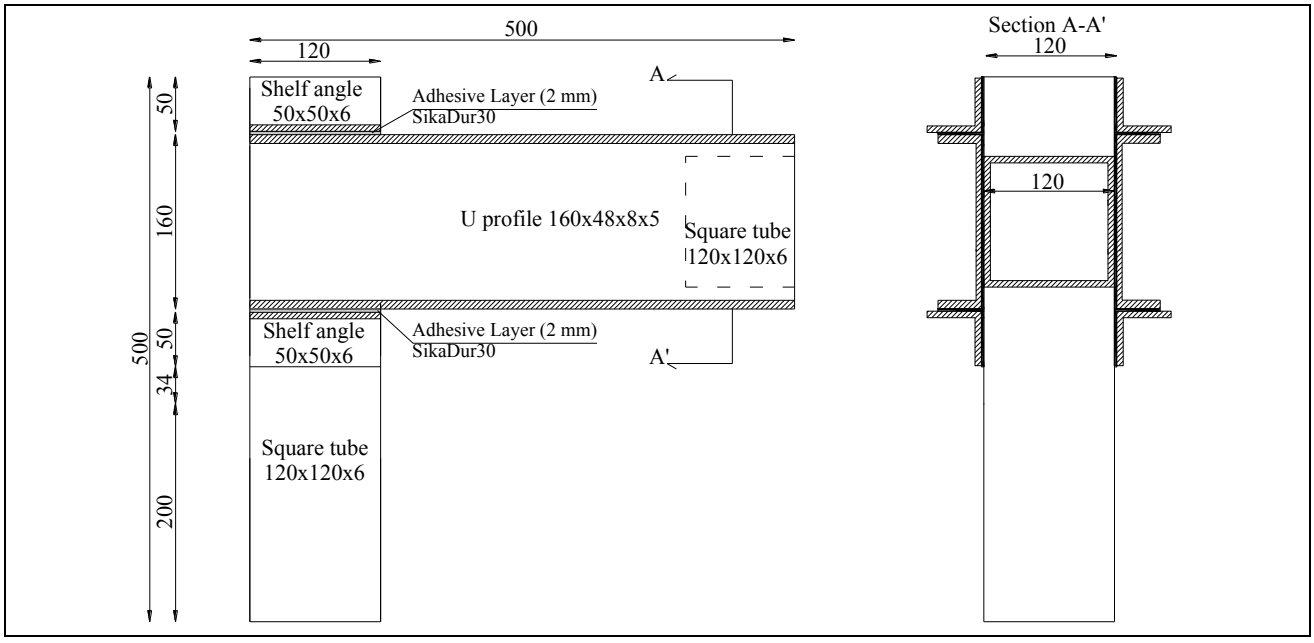

"This is a post-peer-review, pre-copyedit version of an article published in [Composite Structures]. The final authenticated version is available online at https://doi.org/10.1016/j.compstruct.2019.111069

a)	b)

Figure 1. Adhesive connection: a) Lateral view; b) Frontal view.

As shown in Figure 2a, before applying the adhesive, the bonded surfaces were roughened using a sandpaper to improve the bond. All the components were bonded in one go to avoid significant variations in the environmental conditions and inconsistencies between the different adhesive mixes.

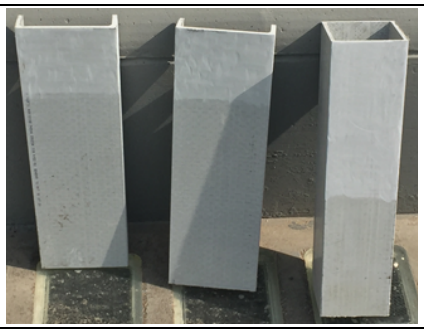

a)	b)

Figure 2. Specimen preparation: a) Sand-coated; b) Assembly.

After the preparation of the specimens, the actual thickness of each of the six adhesive layers was measured in each specimen. The adhesive connections are designated in Figure 3 as AC_*i* (i = 1, 2, ...,10), where AC stands for Adhesive Connection while *i* represents the *i-th* specimen.

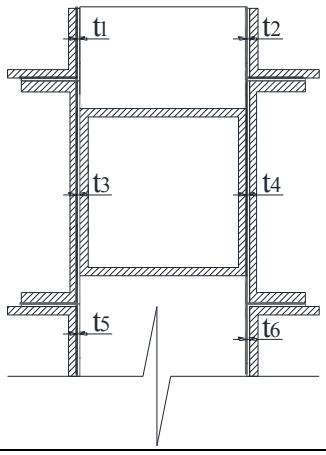

Specimen	t_1	t_2	t_3	t_4	t_5	t_6
#	[mm]	[mm]	[mm]	[mm]	[mm]	[mm]
AC_1	1.0	1.0	1.5	1.5	2.0	2.0
AC_2	1.0	1.0	2.5	2.5	1.5	1.5
AC_3	1.0	1.0	1.5	1.5	2.5	2.5
AC_4	1.0	1.0	1.5	1.5	1.3	1.3
AC_5	1.5	1.5	1.5	1.5	1.0	1.0
AC_6	1.0	1.0	1.5	1.5	1.0	1.0
AC_7	1.0	1.0	2.5	2.5	1.0	1.0
AC_8	1.0	1.0	2.0	2.0	1.0	1.0
AC_9	1.0	1.0	1.5	1.5	1.0	1.0
AC_10	1.3	1.3	2.5	2.5	1.0	1.0

Figure 3. Adhesive layers thicknesses.

2.2 Design and preparation of bolted joints

The bolted connection was designed in compliance with the recommendations of CEN/TC250 [20]. The minimum requirements for design are specified in Table 1, where the quantities that the symbols in the table represent are identified in Figure 4.

"This is a post-peer-review, pre-copyedit version of an article published in [Composite Structures]. The final authenticated version is available online at https://doi.org/10.1016/j.compstruct.2019.111069

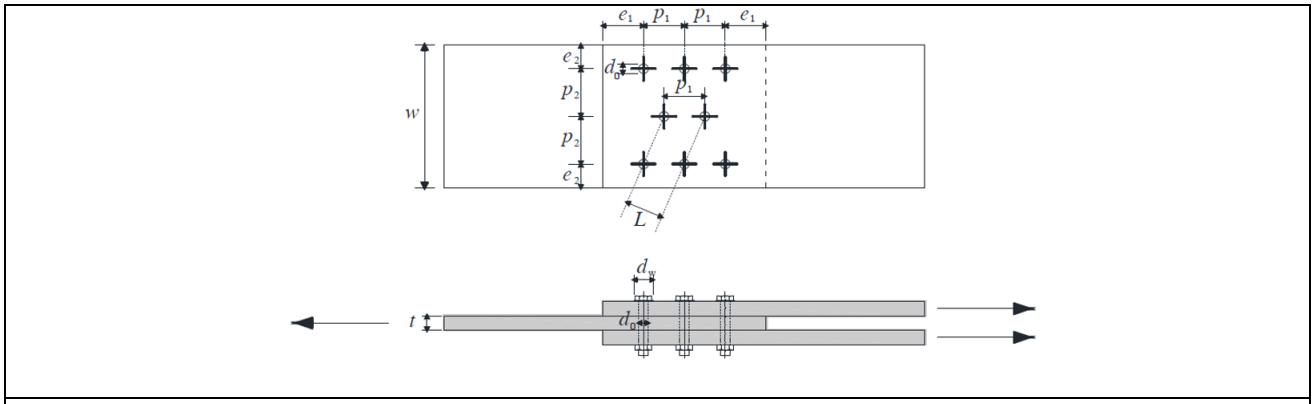

Figure 4. Minimum requirements of joint connection.

Since the minimum thickness of the U-profile web is 6 mm, to satisfy the requirements of CEN TC/250, an 8 mm diameter bolt was selected. The final configuration of the bolted connection, including the location and spacing of the bolt holes, is shown in Figure 5.

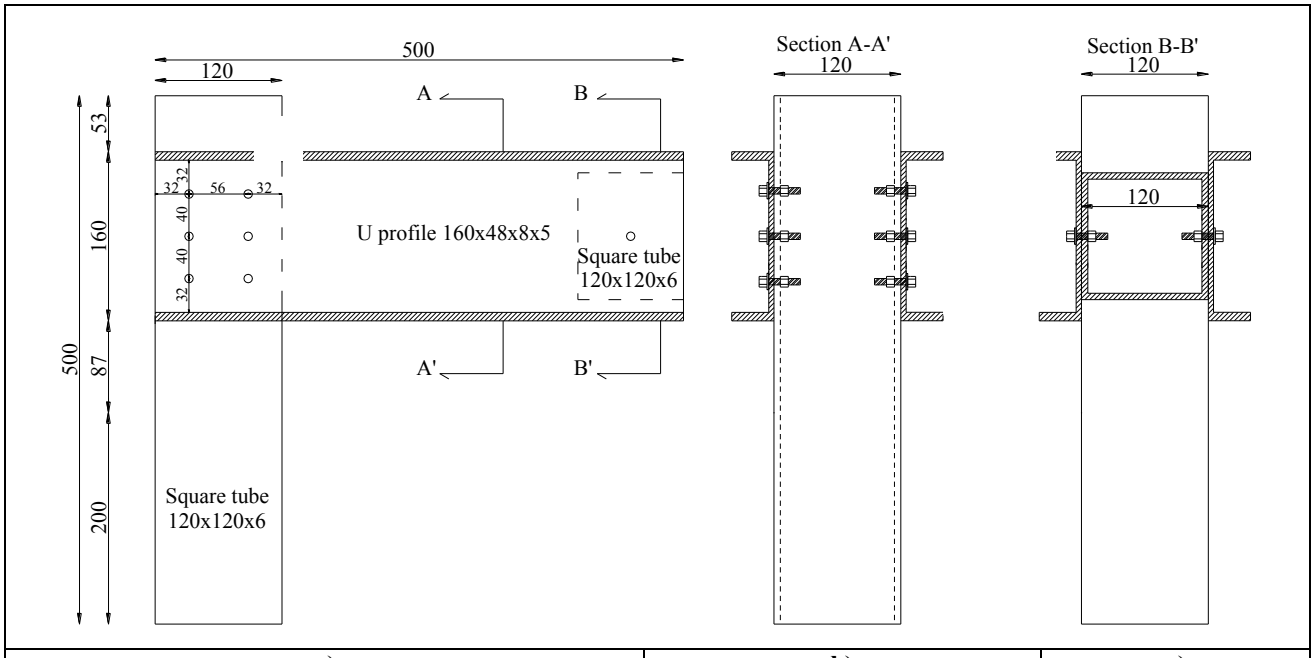

a) **b)** **c)**

Figure 5. Bolted connection: a) Lateral view; b) Frontal view (Section A-A'); c) Frontal view (Section B-B').

The two U-profiles were connected to each other at the free end of the built-up beam by a 100 mm long square tube, similarly to the companion bonded specimens, inserted between the two profiles and bolted to their webs.

Table 1. Minimum requirements for bolted connection geometries (CEN TC/250) [20].

Bolt diameter (d) (recommended range)	$d \geq t_{min}$ ($t_{min} \leq d \leq 1.5\ t_{min}$)
Hole diameter (d_0)	d_0-d ≤ 1 mm
Distances between holes	$p_1 \geq 4d$ $p_2 \geq 4d$ $L \geq 2.8d$
Distances from edges single row multi-rows	side $e_2 \geq 4d$ end $e_1 \geq 4d$ end $e_1 \geq 4d$

Table 2. Design values of material strengths.

"This is a post-peer-review, pre-copyedit version of an article published in [Composite Structures]. The final authenticated version is available online at https://doi.org/10.1016/j.compstruct.2019.111069

Failure-design values		
Pin-bearing		
$V_{Lr,Rd}$	5.00	kN
$V_{Tr,Rd}$	3.00	kN
Net-tension		
$V_{Lr,Rd}$	69.59	kN
$V_{Tr,Rd}$	14.50	kN
Shear-out		
V_{Rd}	8.59	kN
Bolt-shear		
V_{Sd}	14.05	kN

In Table 2 the design values of material strengths for the relevant stress states are reported. For each state, the strength in the longitudinal ($V_{Lr,Rd}$) and transverse ($V_{Tr,Rd}$) direction are reported. Note, the longitudinal direction coincides with the direction of the length of the member.
The bolted connections are designated as BC_*i* (i=1, 2, …,5), where BC stands for Bolted Connection while *i* represents the *i-th* specimen.

2.3 Experimental set-up
Each specimen was loaded by a point load applied near the free end of its built-up beam by means of a rigid steel arm clamped to the testing machine. The test set-up is schematically illustrated in Figure 6a, which shows that the load is applied at distance of 420 mm from the axis of the column. The column was inserted into a steel jacket, and the small gap (1 mm) between the column and the jacket was filled by steel shims. Therefore, the column can be assumed fixed at its basis, with its unsupported length being 300 mm. Further details of the test set-up are provided in Figures 6b and c.

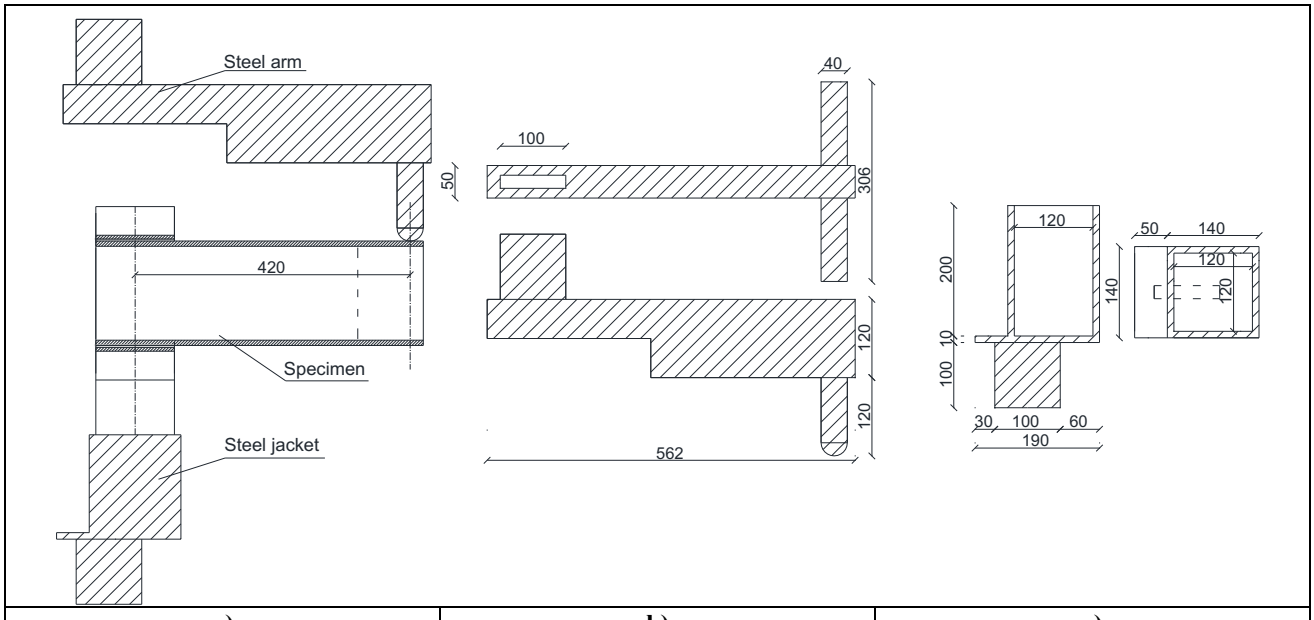

a) **b)** **c)**

Figure 6. Steel elements: a) Schematic view; b) Arm for applying load; c) Jacket.

Figures 7a and 7b show photos of the typical adhesive and bolted connections, respectively, being tested.

"This is a post-peer-review, pre-copyedit version of an article published in [Composite Structures]. The final authenticated version is available online at https://doi.org/10.1016/j.compstruct.2019.111069

a)

b)

Figure 7. Typicall specimen: a) Adhesive; b) Bolted.

As shown in Figure 8, three transducers were used to measure each specimen's vertical (DT1) and horizontal (DT2 and 3) displacements at selected locations and to capture the connection deformations. In addition, twenty strain gauges were installed on each connection, as illustrated in Figure 9, to measure strain distribution on the web of the U-profiles and on the vertical legs of the angles. During each test, all load, displacement and strain values were recorded by means of an automatic data acquisition system comprising two ''System 5100 Vishay MM" switchboards in parallel with 60 extensometric channels. Note, however, that although strain measurements were made, the discussion of the strain values is not germane to the results/conclusions of the current paper.

a)

b)

Figure 8. LVDT position: a) Vertical DT1; b) Horizontal DT2 and DT3.

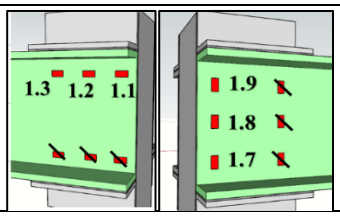

a)

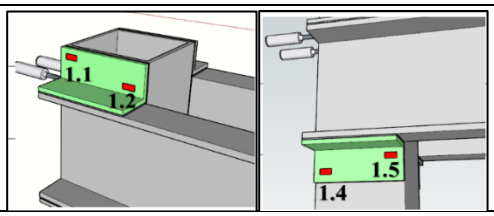

b)

Figure 9. Strain gauges position: a) On the web of the beam; b) On the upper and lower shelf angles.

3. Loading Regimes

The experimental program involved three loading regimes: quasi-static, cyclic and fatigue. Table 3 shows the specimens designation and their associated loading regime. Thirteen specimens were subjected to monotonically increasing quasi-static load up to failure, henceforth referred to as static

tests, three were subjected to high amplitude loading-unloading cyclic load and the remaining two were subjected to variable amplitude fatigue load. Among the statically tested specimens, five replicate adhesive and five otherwise similar bolted specimens were tested to compare their structural behaviour and strength.

The three cyclic load tests were conducted on adhesive connections only, with the number of cycles being 400, 800 and 1200. In all three tests, each load cycled involved increasing the load from 0.5 kN to 14 kN and then unloading back to 0.5 kN. The maximum 14 kN load was 50% of the average failure load for the adhesive connections tested quasi-statically. To avoid the unintended movement of the test specimens during the unloading process, the minimum load was set at 0.5 kN rather than zero. It should be pointed out that the above maximum load is greater than the design strength value evaluated according to Section 2.3.4.1 of CEN/TC 250 [20].The period for each full cycle was 30 seconds, 15 for loading and another 15 for unloading. At the conclusion of the cyclic load tests, to find their residual strength, the specimens were tested to failure under monotonically increasing quasi-static loading.

Table 3. Specimens designation and their loading regime.

Specimen	Static Test	Cyclic Test	Fatigue Test
AC_1	X		
AC_2	X	X	
AC_3	X		
AC_4	X	X	
AC_5	X		
AC_6	X	X	
AC_7			X
AC_8	X		
AC_9	X		
AC_10			X
BC_1	X		
BC_2	X		
BC_3	X		
BC_4	X		
BC_5	X		

AC Adhesive Connection – BC Bolted Connection

Finally, two adhesive specimens were subjected to the fatigue load shown in Figure 10. Each specimen was intended to be subjected to 240 loading and unloading cycles with the minimum load (P') being 0.25 kN and the maximum load being 95% of the average static strength of the adhesive connections, $P_{u,avg,AC}$. As can be seen in Figure 10, the maximum load was 50%, 75%, 85%, and 95% of $P_{u,avg,AC}$ for the 1st, 2nd, 3rd and 4th, 60 cycles, respectively.

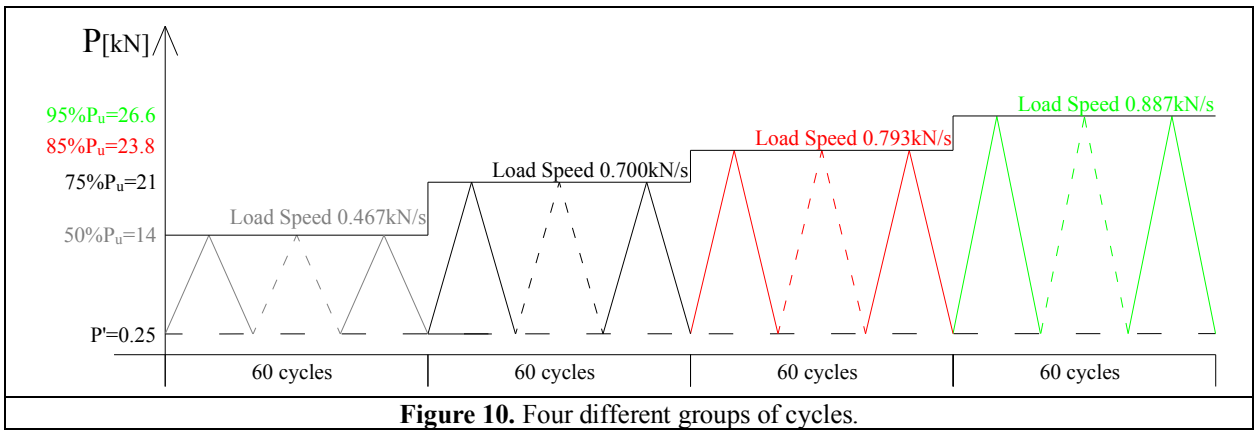

Figure 10. Four different groups of cycles.

"This is a post-peer-review, pre-copyedit version of an article published in [Composite Structures]. The final authenticated version is available online at https://doi.org/10.1016/j.compstruct.2019.111069

4 Test Results

4.1 Static tests: comparison of adhesive to bolted connections

In Figure 11 and 12 the applied load P versus the beam free end vertical displacement δ curves and the moment versus rotation curves are plotted for the specimens with adhesive and bolted connections, respectively. For the adhesive connections, the response is practically linear with slight deviation from linearity near the failure load. Also, except for specimen AC_1, their failure loads and deformations are reasonably close to each other. Specimen AC_1 failed prematurely, albeit still at a higher load than any of the bolted connections. Note that Figures 11b and 12b illustrate the applied moment M acting on the connection versus the relative rotation φ_r between the column and the beam. The M-φ_r curves were computed assuming the beam and the column to be acting as rigid elements due to their short lengths thus the rotation was ascribed to the flexibility of the connection. Furthermore, in Figure 11b, only three curves are shown because in two of the five tests performed on adhesive connections, LVDT DT2 and DT3 malfunctioned and their readings could not be recorded.

The bolted connections exhibit a nonlinear response throughout the loading process until failure. The sudden change in stiffness at the early stages of loading may have been instigated by the loss of frictional resistance between the bolt head and the base material while the subsequent nonlinearity may be a consequence of the bearing stresses acting on bolt holes and the associated hole wall deformations.

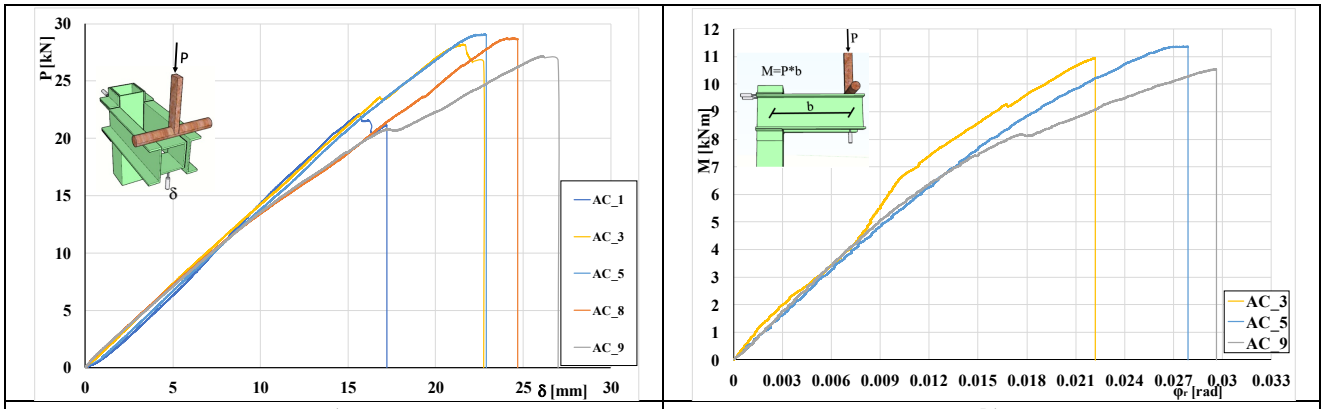

Figure 11. Adhesive connections: a) Load-displacement curves; b) Moment-rotation curves.

In these specimens, failure was initiated by bearing failure, followed by final failure due to shear-out or tear-out. In Figure 12a the design values for bearing failure are shown for the directions parallel (within the column) and perpendicular (within the beam) to the direction of the fibres, which are 5 kN and 3 kN, respectively. The curves in the latter figure exhibit reduction in stiffness between those two load levels.

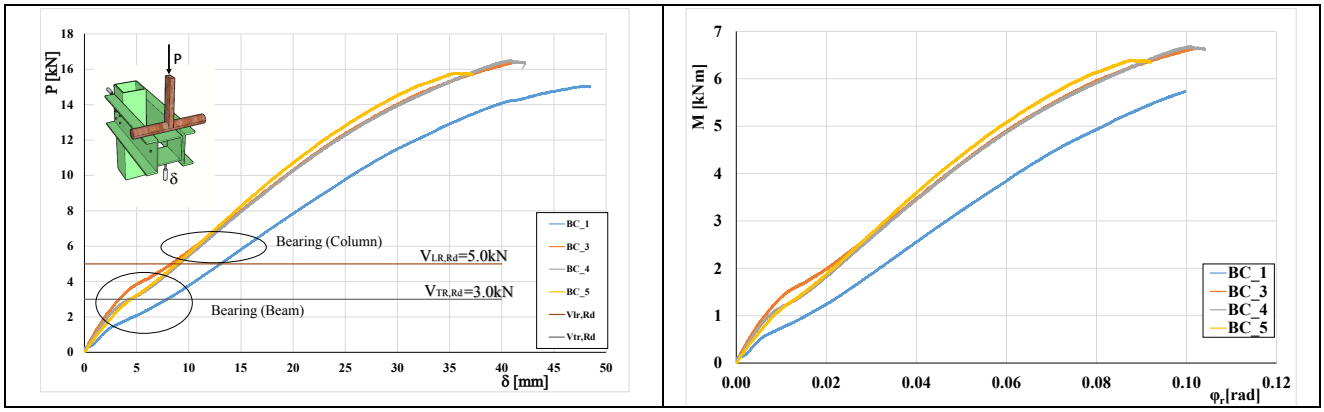

"This is a post-peer-review, pre-copyedit version of an article published in [Composite Structures]. The final authenticated version is available online at https://doi.org/10.1016/j.compstruct.2019.111069

a)	b)
Figure 12. Bolted connections: a) Load-displacement curves; b) Moment-rotation curves.	

In Fig 12b, the M-φ_r curves for the bolted connections are plotted. As stated earlier, the M-φ relationships are based on the assumption that the beam and column act as rigid bodies and the observed rotation is due to the joint flexibility. Strictly speaking, this assumption may not apply to bolted connections due to the relatively high deformations caused by the large bearing stresses acting on the bolt holes. Furthermore, the curves are intended to compare the relative behaviour of the two types of connections rather than deriving quantitative design values.

In Figure 13, the average P-δ and M-φ_r curves of the two types of connection are plotted. It is important to point out that the results for specimen AC_1 were not included in the calculation of the preceding average values because it failed prematurely and is considered to be an outlier. It can be observed that the adhesive connections exhibit significantly higher strength and stiffness than the companion bolted connections. In particular, the average failure load of the adhesive connections ($P_{u,avg,AC}$) is nearly twice that of the bolted connections ($P_{u,avg,BC}$). Similarly, with reference to the P-δ curves, the secant stiffness of the adhesive connections is more than three times the corresponding stiffness of the bolted connections. Based on the M-φ_r curves in Figure 13b, the average secant rotational stiffness of the adhesive connections is more than two times higher than the corresponding stiffness of the bolted connections. Observe in Figure 13b, the average failure moment of the adhesive and bolted connections are designated as $M_{u,avg,AC}$ and $M_{u,avg,BC}$, respectively.

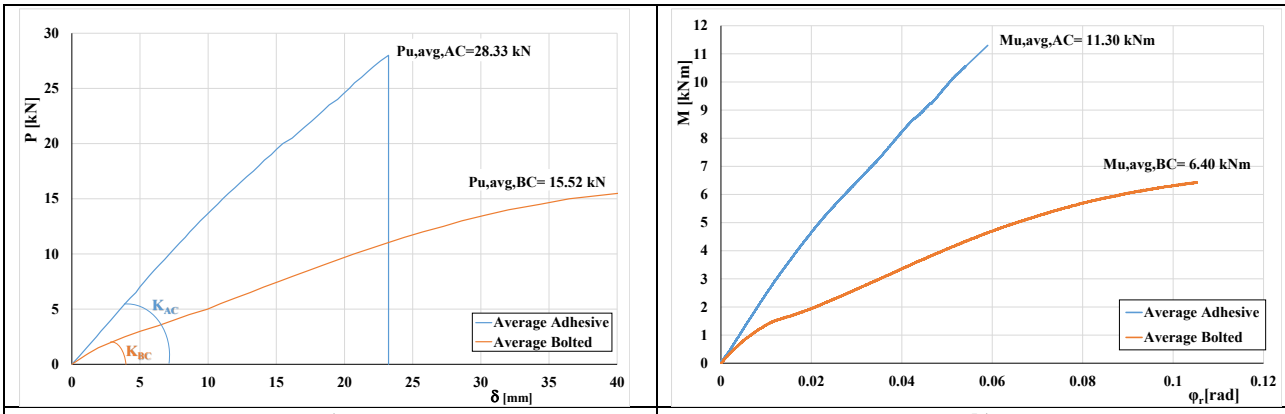

a)	b)
Figure 13. Adhesive vs Bolted connections: a) Average load-displacement curves; b) Average moment-rotation curves.	

Finally, Figure 14 and 15 show pictures of typical failure modes shown by the adhesive and bolted connections, respectively. In particular, Figure 14 shows the expected cohesive failure in the resin (adhesive layer in the web of U-profile) involving the detachment of the mat from the angle profiles. Figure 15 indicates the deformation of the holes which led to large relative rotation between the column and the beam.

"This is a post-peer-review, pre-copyedit version of an article published in [Composite Structures]. The final authenticated version is available online at https://doi.org/10.1016/j.compstruct.2019.111069

Figure 14. Adhesive connections: Cohesive failure mode.

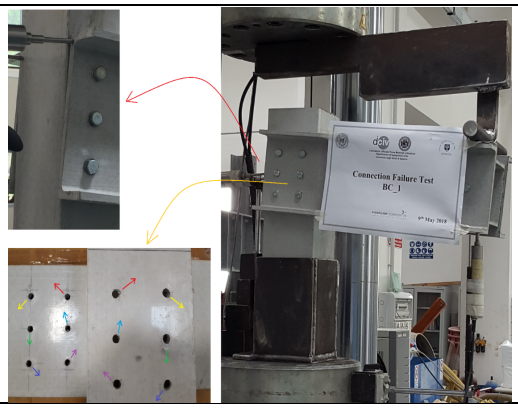

Figure 15. Bolted connections: Pin-bearing failure mode.

4.2 Cyclic load tests: effect on joint stiffness, strength and permanent deformation.

The results of the cyclic load tests on the adhesive connections subjected to 400, 800 and 1200 loading-unloading cycles are presented in Figures 17,18 and 19, respectively.

For the sake of clarity, only curves for the first loading cycle and the last unloading cycle of each specimen are shown, but for completeness actual experimentally obtained graphs, showing the loading and unloading, at the first, 2^{nd}, 5^{th} and 400^{th} cycles for the specimen subjected to 400 cycles are plotted in Figure 16. To avoid crowding and facilitate the current discussion, the graphs for the intermediate cycles are not plotted but they follow a similar trend and fall within the first loading and the last unloading curve. If we consider the loading part of each graph, it is practically a straight line and the lines are virtually parallel from the first to the 400^{th} cycle. On the other hand, the unloading curves for practically all cycles exhibit a bilinear response, with noticeable reduction in stiffness starting at 2 kN. However, upon reloading the specimen recovers its original stiffness, without any noticeable evidence of reduction. We surmise that the observed bilinear response is a consequence of the experimental set-up and some movements were caused by changes in the support condition of the column rather than changes in the characteristics of the GFRP material or the beam-column connection mechanical properties. As will be seen later, the post-cyclic load static test results on these specimens did not show any reduction in their strength or stiffness compared to the companion specimens subjected to static load alone. The above observations also apply to the other two specimens subjected to 800 and 1200 cycles, respectively. For these reasons, in the ensuing discussion only the first and last loading cycle graphs will be plotted and discussed.

With reference to Figures 17 to 19, the straight lines are a close approximation of the actual experimental curves, and it may be noticed that in all three cases there is negligible reduction in the specimen stiffness between the first and last loading cycle. The apparent small hysteresis may be a consequence of the specimen seating after the first application of the load or of the unrecoverable creep but is negligible irrespective of its source.

"This is a post-peer-review, pre-copyedit version of an article published in [Composite Structures]. The final authenticated version is available online at https://doi.org/10.1016/j.compstruct.2019.111069

The values of the beam end permanent vertical displacement, vpd, joint permanent rotation, pm, and specimen stiffness, based on beam free end displacement, K_δ and joint rotation, K_φ, are also given in Figures 17, 18, and 19 for each of the tested specimens. The values of vpd and pm were calculated by subtracting the displacement (rotation) of the first cycle from that of the last cycle. The retention of practically constant stiffness, irrespective of the number of load cycles, indicates lack of damage incurred by the test specimens due to the applied cyclic loads. This observation is confirmed by the results of the static tests performed on them. Figure 20 shows the P-δ and M-φ_r curves of the above specimens resulting from their post-cyclic load static tests and the corresponding curves for the companion specimens that were only statically tested. All the curves fall within a narrow band, well within the expected range due to random variabilities, but there is no evidence that the cyclic loading caused systematic reduction in the strength or stiffness of the relevant specimens.

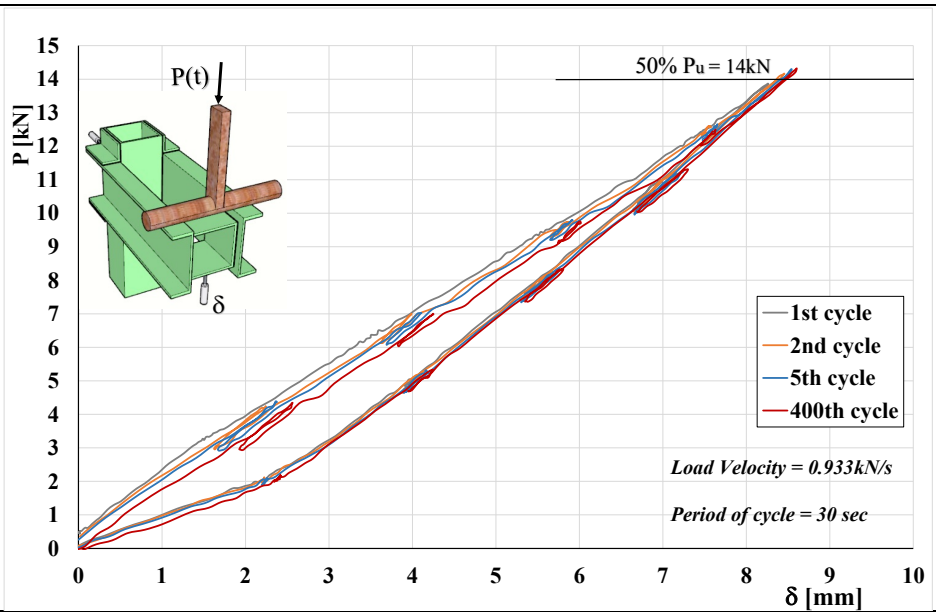

Figure 16. Adhesive connections cyclic test (400 cycles): P-δ curves.

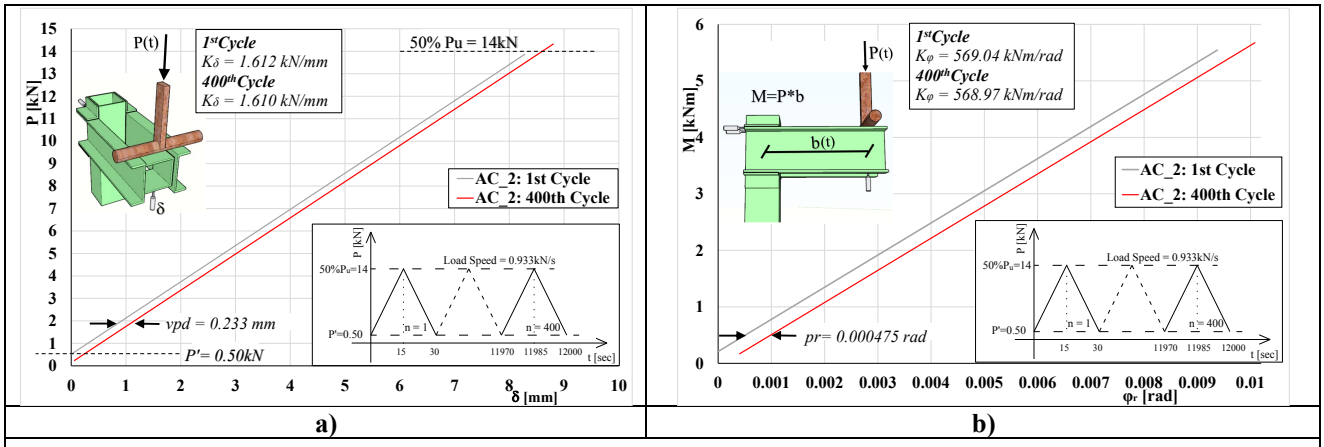

Figure 17. Adhesive connections cyclic test (400 cycles): a) P- δ; b) M-φ_r curves.

"This is a post-peer-review, pre-copyedit version of an article published in [Composite Structures]. The final authenticated version is available online at https://doi.org/10.1016/j.compstruct.2019.111069

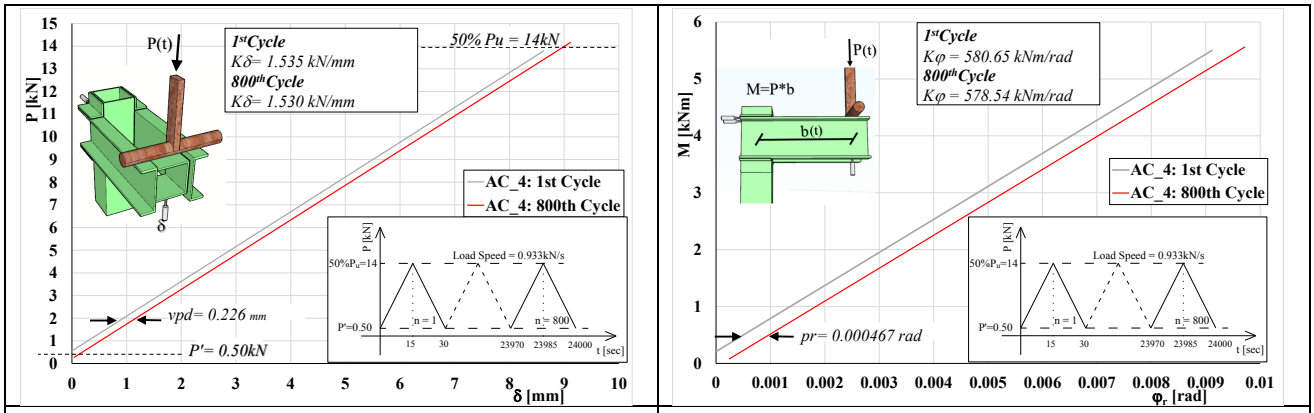

a) b)

Figure 18. Adhesive connections cyclic test (800 cycles): a) P-δ; b) M-φ_r curves.

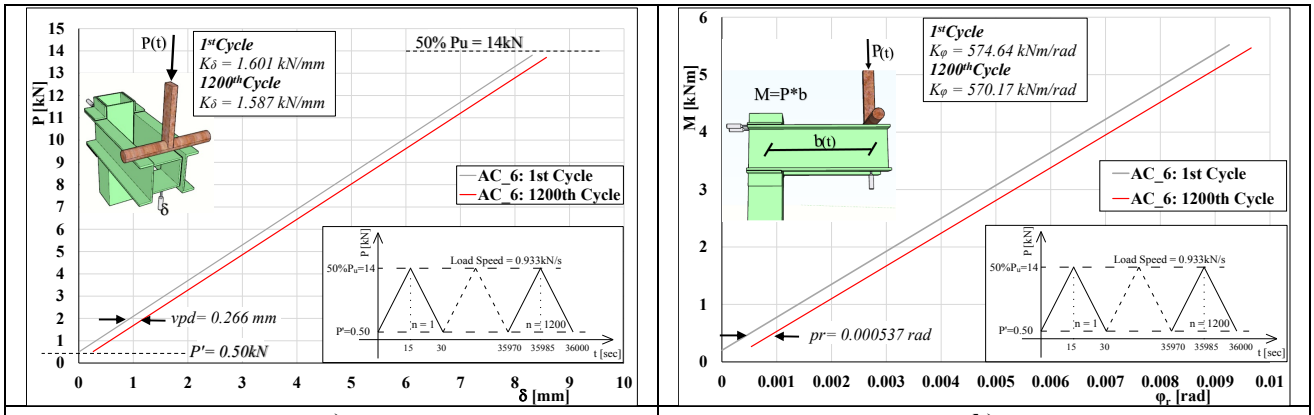

a) b)

Figure 19. Adhesive connections cyclic test (1200 cycles): a) P-δ; b) M-φ_r curves.

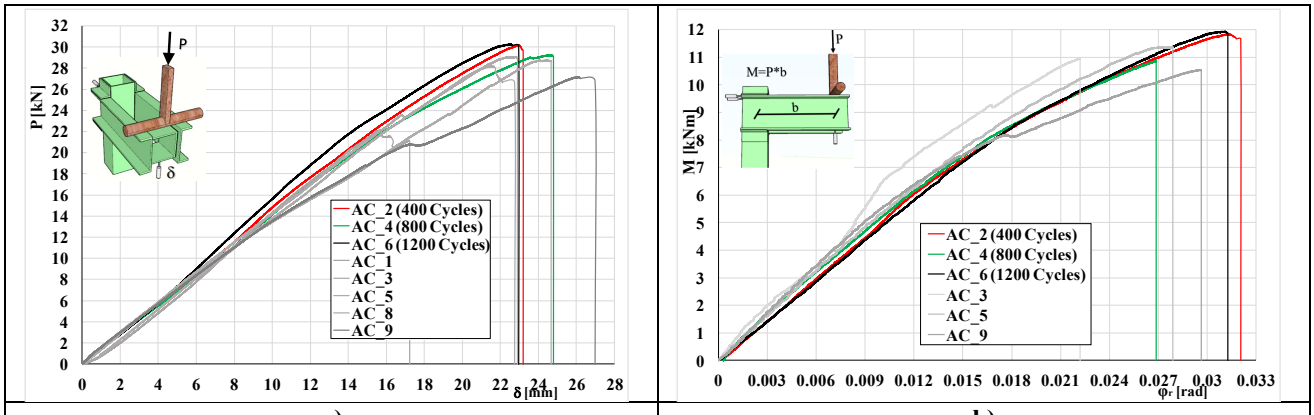

a) b)

Figure 20. The specimens tested cyclically were tested monotonically: a) P-δ curves; b) M-φ_r curves.

4.3 Fatigue tests: effect on connection behaviour and strength.

It may be recalled that the two specimens, AC_7 and AC_10, with adhesive connection were subjected to fatigue loading involving loading-unloading with increasing load amplitude after each 60 load cycles (see Figure 10).

The P-δ and M-φ_r curves for these specimens are plotted in Figures 21 and 22, respectively. Also, the vpd, pm, K_δ and K_φ, of each connection are given in Table 4a-b. Once again, the first cycle loading curve and the last cycle unloading curve corresponding to each load amplitude are shown. Notice that the first cycle loading curve for the 2nd, 3rd and 4th load amplitudes coincides with the

last cycle unloading curve of the preceding load amplitude.
These figures show that up to nearly the end of the third load amplitude, the connections suffered only minor reduction in stiffness but after the application of the load with the 4th amplitude, the stiffness dropped substantially. This reduction was instigated by the appearance of cracks in the adhesive layer between the column face and the lower shelf angle towards the end of the 3rd load amplitude cycles and the subsequent extension and opening of the cracks under the load with the 4th amplitude. As a result of these cracks, specimen AC_7 failed after 16 cycles of the load with the 4th amplitude while AC_10 failed after 24 cycles of the same load amplitude. It is, however, interesting to notice that despite the appearance of the cracks, these specimen remained linear elastic throughout the loading and unloading cycles up to failure. This may be that the cracks remained stable after their initial opening and did not further propagate until their sudden extension at failure (see Figure 23).

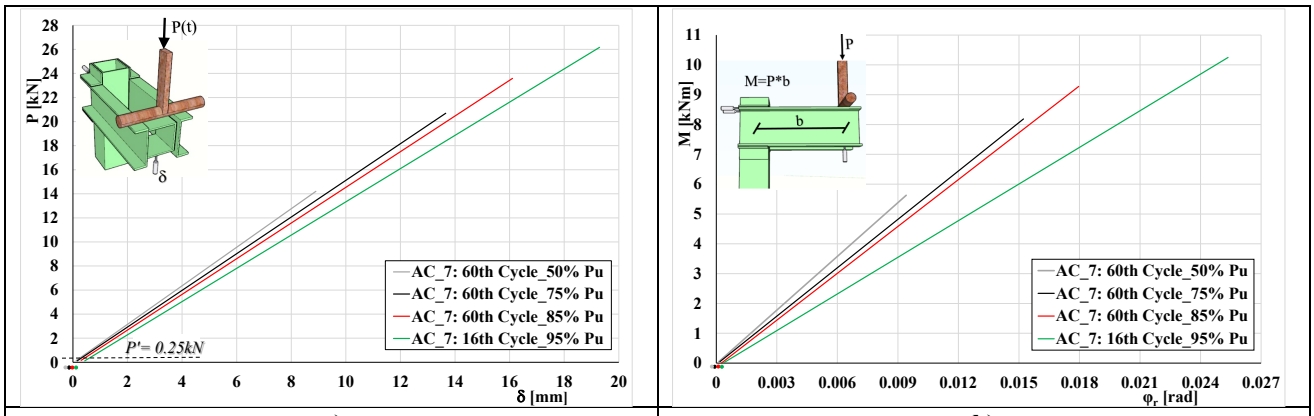

a) b)

Figure 21. Fatigue tests on AC_7 varying load level: a) P-δ; b) M-φ_r curves.

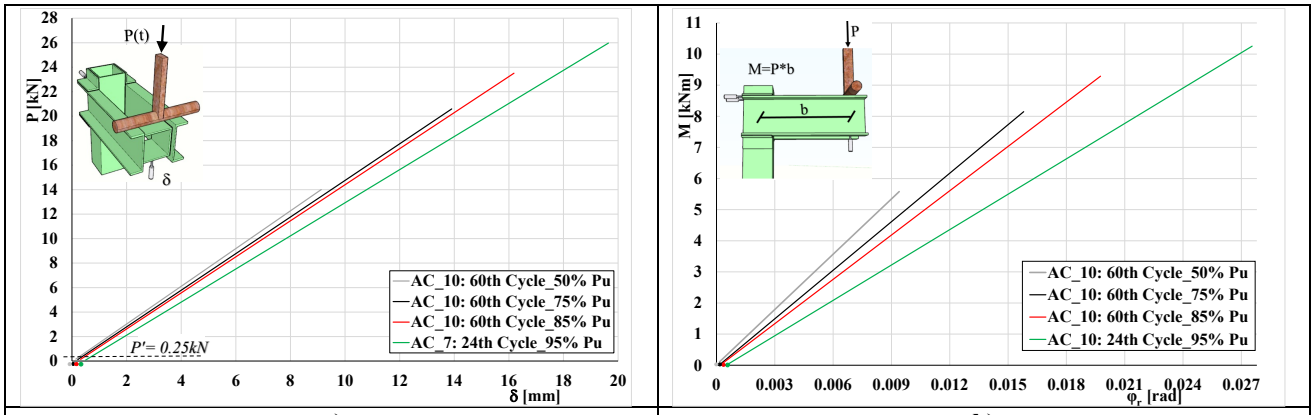

a) b)

Figure 22. Fatigue tests on AC_10 varying load level: a) P-δ; b) M-φ_r curves.

"This is a post-peer-review, pre-copyedit version of an article published in [Composite Structures]. The final authenticated version is available online at https://doi.org/10.1016/j.compstruct.2019.111069

Figure 23. Delamination observed at 85% of the ultimate load P_u.

Table 4a. Specimen stiffness based on beam free end displacement, K_δ, and permanent vertical displacement, vpd, for several load level.

Specimen	50%Pu		75%Pu		85%Pu		95%Pu		$\frac{K_{\delta,50}-K_{\delta,95}}{K_{\delta,95}}$	Σvdp
	K_δ [kN/mm]	vpd [mm]	K_δ [kN/mm]	vpd [mm]	K_δ [kN/mm]	vpd [mm]	K_δ [kN/mm]	vpd [mm]	[%]	[mm]
AC_7	1.601	0.118	1.534	0.041	1.483	0.145	1.381	0.132	15.93	0.436
AC_10	1.541	0.141	1.495	0.070	1.472	0.104	1.352	0.183	13.98	0.498

Table 4b. Specimen stiffness based on joint rotation, K_φ, and permanent rotation, pr, for several load level.

Specimen	50%Pu		75%Pu		85%Pu		95%Pu		$\frac{K_{\varphi,50}-K_{\varphi,95}}{K_{\varphi,95}}$	Σpr
	K_φ [kN/mm]	pr [mm]	K_φ [kN/mm]	pr [mm]	K_φ [kN/mm]	pr [mm]	K_φ [kN/mm]	pr [mm]	[%]	[mm]
AC_7	600.45	0.000123	561.01	0.000057	543.45	0.000074	439.61	0.000105	36.59	0.000359
AC_10	589.01	0.000154	549.01	0.000068	514.73	0.00084	442.55	0.000284	33.09	0.000590

4. Comparison with results of previous adhesive joint tests

To gauge the superior performance of the adhesive connection investigated in the current study against those of other types of adhesive connections previously investigated by the current authors, reference can be made to Table 5. Details of the previously tested connections can be found in Ascione et al. [19,21]. In the latter case, a 200x100x10mm GFRP I-profile was used to make the beam and column and they were adhesively connected using either GFRP shelf angles [19] or shelf angles plus CFRP wrap [21]. The test setup was similar to the one in the current investigation and all specimens were loaded quasi-statically to failure.

"This is a post-peer-review, pre-copyedit version of an article published in [Composite Structures]. The final authenticated version is available online at https://doi.org/10.1016/j.compstruct.2019.111069

Table 5 shows for each specimen its failure load (P_u), observed failure moment (M_u), its theoretical bending capacity moment capacity (M_{th}) and the ratio $\eta(\%) = \left(M_u / M_{th}\right) x100$, which can be interpreted as the connection efficiency. Note, the moment M_{th} was computed using the conventional flexure formula and the assumption of linear elasticity.

Table 5. Comparison between adhesive connection types tested by the authors.

Connection	**Type**	**Source**	**Average Failure load, P_u** [kN]	**Average Failure moment, M_u** [kNm]	**Profile Theoretical Moment Capacity, M_{th}** [kNm]	$\eta = \frac{M_u}{M_{th}} \times 100$ [%]
Adhesive	BTCJ_fcr	[19]	22.50	10.15	55.80	18.19
Adhesive	BTCJ_fcww	[21]	21.00	10.15	55.80	18.19
Adhesive	AC	present study	28.90	11.40	33.96	33.56

It is important to mention that the average failure load and monent in the last row of Table 5 are computed by averaging the relevant values for the four quasi-statically loaded specimens plus the results of static tests carried out on specimens after being subjected to cyclic loading.

It is clear from the results in the last table that the present connection achieved the highest failure load and moment as well as the highest efficiency. The efficiency of the current connection is 84.4% higher than the best performing I-beam connection tested previously.

5. Conclusions

A GFRP hollow square section, serving as a column, was connected to a built-up beam made of two U-profiles by means of either an epoxy adhesive and GFRP shelf angles or steel bolts. The beam-column assembly formed an L-shaped frame which was tested by applying a point load at the beam free end while the column was fixed at its base. Both types of connections were subjected to monotonically increasing quasi-static loading up to failure. Additional adhesive connections were also subjected to either cyclic or fatigue type loading. The results of the study support the following conclusions:

1. Under quasi-static loading, the adhesive connection exhibited on average 82% higher load than the companion bolted connection.
2. The adhesive connection had a secant stiffness, based on the beam displacement, that was over 300% larger than that of the companion bolted connection.
3. The adhesive connection secant rotational stiffness was on average more than 380% higher than that of the companion bolted connection.
4. The adhesive connection failure moment was 33.5% of the ultimate moment capacity of the beam. This value is at least 80% higher than any other connection tested in the past.
5. The application of up to 1200 loading and unloading cycles with amplitude equal to 50% of the average static load capacity of the adhesive connection had negligible effect on its strength or stiffness.
6. The adhesive connection could sustain at least 196 cycles of loading and unloading with

"This is a post-peer-review, pre-copyedit version of an article published in [Composite Structures]. The final authenticated version is available online at https://doi.org/10.1016/j.compstruct.2019.111069

increasing amplitude after each 60 cycles, with the highest amplitude equal to 0.95 $P_{u,av}$, in the last 16 cycles. The connection stiffness exhibited minor reduction up to the first 120 cycles, but after being subjected to another 60 cycles of a load with amplitude of 0.85 $P_{u,av,}$ it experienced some cracks in the adhesive layer accompanied by significant reduction in stiffness. However, the crack remained stable and the connection was able to sustain another at least 16 cycles of a load with amplitude of 0.95 $P_{u, av}$.

7. The results of the current investigation show that under short-term loading the current adhesive connection can achieve higher strength and stiffness than any other reported connection in GFRP members, but further investigation is required to determine its long-term performance under sustained load and variable humidity and temperature conditions.

Acknowledgments

The authors thank the Fiberline Ltd. for providing the materials. They would also like to thank Messrs Aniello Casillo and Michele Palumbo, master's students at the Department of Civil Engineering at the University of Salerno, for their assistance during the preparation and testing of the specimens. Special thanks to the State Administration of Foreign Experts of China, the Tianjin Municipal Government and Nankai University for their financial support of this research collaboration.

References

[1] Correia JR. GFRP pultruded profiles in civil engineering: hybrid solutions, bonded connections and fire behaviour, PhD thesis in civil engineering, Instituto Superior Técnico, Technical University of Lisbon; 2008.

[2] Carra G, Carvelli V. Long-term bending performance and service life prediction of pultruded glass fibre reinforced polymer composites. Compos Struct 2015; 127:308–315.

[3] Machado JJM, Marques EAS, da Silva LFM. Influence of low and high temperature on mixed adhesive joints under quasi-static and impact conditions. Compos Struct 2018; 194:68–79.

[4] Liao K, Schultheisz CR, Hunston DL. Effects of environmental aging on the properties of pultruded GFRP. Compos B Eng 1999;30(5):485–93.

[5] Cabral-Fonseca S, Correia JR, Rodrigues MP, Branco FA. Artificial accelerated ageing of GFRP pultruded profiles made of polyester and vinylester resins: characterization of physical-chemical and mechanical damage. Strain 2012;48(2):162–73.

[6] Mara V, Haghani R, Harrysin P. Bridge decks of fibre reinforced polymer (FRP): a sustainable solution. Constr Build Mater 2014;50:190–9.

[7] Minghini F, Tullini N, Laudiero F. Vibration analysis of pultruded FRP frames with semi-rigid connections. Eng Struct 2010; 32:3344-3354.

[8] Manalo A, Aravinthan T, Fam A and Benmokrane B. State-of-the-Art Review on FRP Sandwich Systems for Lightweight Civil Infrastructure. Compos Constr 2017, 21(1).

[9] Bank LC, Mosallam AS, McCoy GT. Design and performance of connections for pultruded frame structures. Reinf Plast Compos 1994;15:1052–67.
[10] Mosallam AS, Abdelhamid MK, Conway JH. Performance of pultruded FRP connections under static and dynamic loads. Reinf Plast Compos 1994;13:386–407.
[11] Bank LC, Yin J, Moore L. Experimental and numerical evaluation of beam-to-column connections for pultruded structures. Reinf Plast Compos 1996;15:1052–67.
[12] Smith SJ, Parsons ID, Hjelmstad KD. An experimental study of the behaviour of connections for pultruded GFRP I-beams and rectangular tubes. Compos Constr 1998;42:281–90.
[13] Smith SJ, Parsons ID, Hjelmstad KD. Experimental comparisons of connections for GFRP pultruded frames. Compos Constr 1999;3:20–6.
[14] Mottram JT, Zheng Y. Further tests on beam-to-column connections for pultruded frames: web-cleated. Compos Constr 1999;3:3–11.
[15] Mottram JT, Zheng Y. Further tests of beam-to-column connections for pultruded frames: flange-cleated. Compos Constr 1999;3:108–16.
[16] Qureshi J, Mottram JT. Behaviour of pultruded beam-to-column joints using steel web cleats. Thin-Walled Struct 2013;73:48–56.
[17] Qureshi J, Mottram JT. Response of beam-to-column web cleated joints for FRP pultruded members. Compos Constr 2014;18.
[18] Mosallam AS. Design guide for FRP composite connections, Manual of practice (MOP) 102, ASCE 2011, Reston, VA, 624.
[19] Ascione F, Lamberti M, Razaqpur AG, Spadea S. Strength and stiffness of adhesively bonded GFRP beam-column moment resisting connections. Compos Struct 2017;160:1248–57.
[20] Report EUR 27666 EN (CEN TC/250). Prospect for new guidance in the design of FRP. JRC Science for Policy Report (https://ec.europa.eu/jrc/en/publication/eur-scientific-and-technical-research-reports/prospect-new-guidance-design-frp).
[21] Ascione F, Lamberti M, Razaqpur AG, Spadea S, Malagic M. Pseudo-ductile failure of adhesively joined GFRP beam-column connections: An experimental and numerical investigation. Compos Struct 2018;200:864–873.
[22] Wu C, Zhang Z, Bai Y. Connections of tubular GFRP wall studs to steel beams for building construction. Compos B Eng 2016, 95, 64-75.
[23] Zhang Z, Wu C, Nie X, Bai Y and Zhu L. Bonded sleeve connections for joining tubular GFRP beam to steel member: Numerical investigation with experimental validation. Compos Struct 2016, 157, 51-61.
[24] Zhang ZJ, Bai Y, Xiao, X. Bonded Sleeve Connections for Joining Tubular Glass Fiber–Reinforced Polymer Beams and Columns: Experimental and Numerical Studies. Compos Constr 2018, 22(4), 04018019.
[25] Zhang Z, Bai Y, He X, Jin L, Zhu L. Cyclic performance of bonded sleeve beam-column connections for FRP tubular sections. Compos B Eng 2018.
[26] Martins D, Correia JR, Gonilha J, Arruda M, Silvestre N. Development of a novel beam-to-column connection system for pultruded GFRP tubular profiles. Compos Struct 2017;171:263–76.
[27] Fiberline handbook. http://www.fiberline.com.
[28] SikaDur30 technical data sheet (2017) ita.sika.com.

"This is a post-peer-review, pre-copyedit version of an article published in [Composite Structures]. The final authenticated version is available online at https://doi.org/10.1016/j.compstruct.2019.111069